

## Effects of ozone and well-mixed gases on annual-mean stratospheric temperature trends

V. Ramaswamy and M. D. Schwarzkopf

NOAA/Geophysical Fluid Dynamics Laboratory, Princeton University, Princeton, New Jersey, USA

Received 6 June 2002; revised 5 July 2002; accepted 17 July 2002; published 27 November 2002.

[1] The effects of changes in ozone and well-mixed greenhouse gases upon the annual-mean stratospheric temperatures are investigated using a general circulation model and compared with the observed (1979–2000) trends. In the global-mean lower stratosphere (50–100 hPa), ozone changes exert the most important influence upon the cooling trend. In the upper stratosphere, where both ozone and greenhouse gas changes influence the temperature trends, the amount of cooling is sensitive to the background ozone climatology. Taking into account the uncertainties in the observed temperature trend estimates and the dynamical variability of the model, the simulated results are in reasonable quantitative agreement with the vertical profile of the observed global-and-annual-mean stratospheric cooling, and with the observed lower stratospheric zonal-and-annual-mean cooling. This affirms the major role of these species in the temperature trend of the stratosphere over the past two decades. *INDEX TERMS:* 3359 Meteorology and Atmospheric Dynamics: Radiative processes; 1610 Global Change: Atmosphere (0315, 0325); 1620 Global Change: Climate dynamics (3309). **Citation:** Ramaswamy, V., and M. D. Schwarzkopf, Effects of ozone and well-mixed gases on annual-mean stratospheric temperature trends, *Geophys. Res. Lett.*, 29(22), 2004, doi:10.1029/2002GL015141, 2002.

### 1. Introduction

[2] General circulation model (GCM) investigations indicate that the stratospheric temperature structure is sensitive in general to changes in trace gas concentrations [Ramaswamy *et al.*, 2001, hereinafter R01]. Changes in well-mixed greenhouse gases (WMGGs), ozone and water vapor [Hansen *et al.*, 1995; Ramaswamy *et al.*, 1996, hereinafter RSR; Forster and Shine, 1999, hereinafter FS; Langematz, 2000, hereinafter L; Rosier and Shine, 2000, hereinafter RS] have been shown to exert substantial perturbations to the stratospheric climate. Here, we perform simulations with a GCM to investigate the consequences of the observed changes in the WMGGs and ozone over the last two decades upon stratospheric temperatures, and diagnose their relative roles in the lower, middle and upper stratosphere. We examine the sensitivity of the results to the background stratospheric ozone climatology, and compare the simulated results with the recent compilation of the observed annual-mean temperature trends (R01). We consider the results in the light of uncertainties in observed trend estimates and that arising due to the model's dynamical variability, and thus evaluate the extent to which ozone and WMGGs can account for the observed trends.

### 2. Model and Observations

[3] The model employed is the Geophysical Fluid Dynamics Laboratory (GFDL) "SKYHI" GCM with  $3 \times 3.6^\circ$  resolution in latitude and longitude and 40 vertical layers [Ramachandran *et al.*, 2000], but with the upper stratospheric ozone amounts not varying with temperature. Monthly-mean sea-surface temperatures are prescribed based on climatological values. The stratospheric ozone trends data are from Randel and Wu [1999]. The ozone changes extend from 50 km down to  $\sim 20$  km in the tropics,  $\sim 13$  km in midlatitudes, and  $\sim 10$  km in polar regions.

[4] The standard SKYHI model ozone climatology [Fels *et al.*, 1980] is based upon knowledge of ozone distribution and ozone-temperature linkages known in the early 1970s. Since the sensitivity to the choice of the background ozone climatology has not been explicitly considered previously, we consider two climatologies, one being the standard SKYHI climatology and the other a climatology based on the 1989–1991 ozone data [Fortuin and Kelder, 1998, hereinafter FK]. The main difference between the two climatologies is that the latter generally has less ozone in the lower stratosphere but more in the upper stratosphere.

[5] Two sets of GCM experiments are performed. "Set A" employs the standard SKYHI ozone climatology. The zonal and monthly-mean ozone loss over the 1979–1997 period is applied to this background profile to obtain the corresponding perturbation ozone profile. "Set B" employs the FK climatology. In this set, the 1979 (unperturbed) monthly-mean ozone profile is the sum of the FK climatology and the ozone trends, evaluated retrospectively for 11 years; the 1997 monthly ozone profile is the sum of the FK climatology and the trend profile, evaluated prospectively for 7 years. For "Set A", two perturbation simulations are conducted - one (A1) with ozone changes alone, the second (A2) with ozone plus WMGG changes. Similar simulations are performed in the "Set B" framework, with B1 denoting the ozone-only and B2 the ozone plus WMGG simulations. Each perturbation simulation is run for 21 model years. The averages from the last 20 years are compared to those from the appropriate 20-year unperturbed run to obtain the response.

[6] The WMGG species include CO<sub>2</sub>, CH<sub>4</sub>, N<sub>2</sub>O, CFC11, CFC12, CFC113 and HCFC22; each is assumed to be uniformly mixed. For the unperturbed run and the ozone-only change experiments (A1 and B1), the 1980 WMGG concentrations are employed; experiments A2 and B2 use the 1997 values (IPCC, 1996). The standard deviation of the simulated temperature is estimated from the 20-year integrations with unperturbed profiles and is similar in both sets. The observations employed are the decadal temperature trends obtained from the MSU (Channel 4) and SSU (15X) instruments (R01; J. Austin, personal communication), updated for

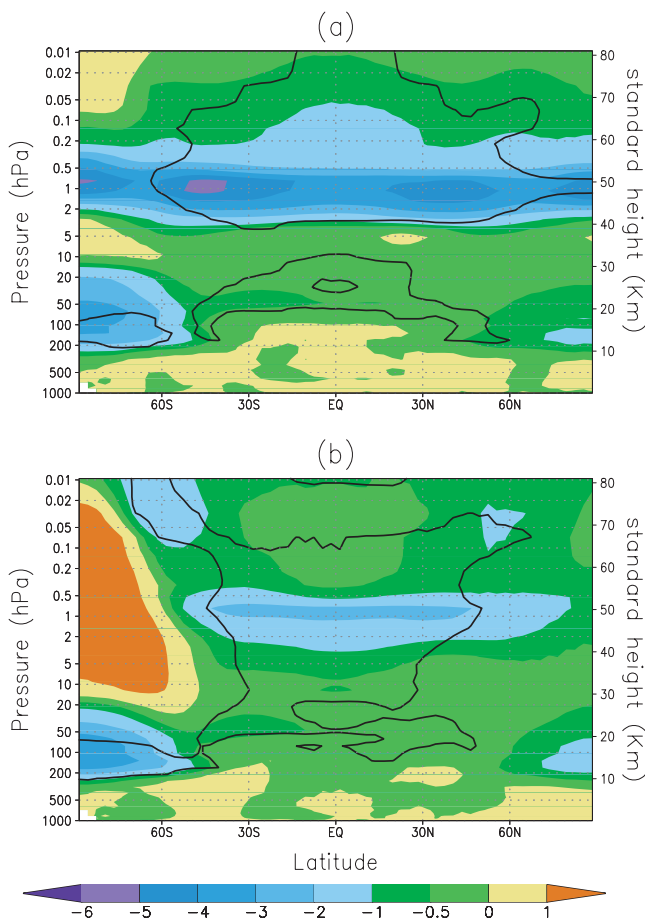


**Figure 1.** Stratospheric temperature change due to observed ozone depletion (1979–1997) from (a) A1 and (b) B1 simulations. Solid lines denote statistical significance (95% confidence level of a student t- test).

the period 1979–2000. The atmospheric emission sensed by these instruments comes from a wide range in altitude (R01).

### 3. Simulation Results

[7] The zonal-mean change in the stratospheric temperatures over the simulated period resulting from the A1 and B1 experiments (Figure 1) exhibits a cooling of the lower stratosphere ( $\sim 50$ – $100$  hPa) at all latitudes, with peak cooling in the Antarctic (exceeding 3K); a region of generally lesser cooling (or even a warming) above the lower stratosphere; and strong cooling in the upper stratosphere (except over the Antarctic in B1), peaking at  $\sim 1$  hPa. These features are broadly consistent with the patterns in RS and L. The Antarctic stratospheric warming, which is spread over a greater area in B1, stems from a change in the dynamical circulation resulting in compressional heating above regions of ozone depletion [Mahlman *et al.*, 1994; RSR; L; RS]. In both sets, statistical significance is obtained in the low-to-mid-latitude upper stratosphere, in portions of the low-latitude middle and lower stratosphere, and over a major portion of the Antarctic lower stratosphere. The results in the northern polar lower and middle stratosphere are statistically insignificant owing to the large dynamical variability in this region, a feature also evident in observations [Labitzke and van Loon, 1995].

[8] The major difference between the two results is the magnitude of cooling above  $\sim 5$  hPa. In the low latitudes, A1 has a lesser cooling at  $\sim 5$  hPa than B1 but then a more rapid increase of the cooling trend with height, such that the trend at  $\sim 1$  hPa is about twice that in B1. The A1 result is substantially different from the results of L and RS, while the B1 result is closer to these studies. To explain the difference between A1 and B1, we note that, in the upper stratosphere, the temperature is maintained primarily by a balance between absorption of ultra-violet (UV) radiation by ozone and long-wave cooling due to the  $15 \mu\text{m}$   $\text{CO}_2$  band [Fels *et al.*, 1980, Appendix B]. Then, a radiative perturbation due to ozone change ( $\delta r_{\text{O}_3}$ ) yields a temperature change ( $\delta T$ ) as:

$$\delta T \propto T^2 \exp(960/T) \delta Q_{\text{sw}}(r_{\text{O}_3}, \delta r_{\text{O}_3}) \quad (1)$$

[9] The temperature change thus depends on the short-wave radiative “drive” ( $\delta Q_{\text{sw}}$ ) and the unperturbed temperature ( $T$ ).  $\delta Q_{\text{sw}}$  depends on the background ozone profile ( $r_{\text{O}_3}$ ) owing to the nonlinear dependence of UV radiation absorption on the ozone amount, with the change in absorption per unit ozone change decreasing as ozone amount increases. The visible solar absorption by ozone, in contrast, has a linear dependence on the ozone amount. From Lacis and Hansen [1974, Equation (9)], for a similar change in upper stratospheric ozone, we can write:

$$[\delta Q_{\text{sw}}(r_{\text{O}_3, \text{A}}, \delta r_{\text{O}_3})] / [\delta Q_{\text{sw}}(r_{\text{O}_3, \text{B}}, \delta r_{\text{O}_3})] \propto \{x_{\text{O}_3, \text{B}} / x_{\text{O}_3, \text{A}}\}^{0.8} \quad (2)$$

where  $x$  is the ozone column amount from the top of the atmosphere. Since the background ozone in B1 is almost twice that of A1 at  $\sim 1$  hPa, the shortwave drive in B1 is smaller, and the expected temperature change is about half of that in A1. In addition, the simulations show that the increased background ozone in B1 (and thus increased ozone heating) results in a  $\sim 10\text{K}$  increase in the unperturbed equilibrium temperature at  $\sim 1$  hPa. From (1), this increase further reduces the expected temperature change, given the same radiative drive; here, this effect is much less important.

[10] The zonal-mean temperature changes from the A2 and B2 experiments are illustrated in Figure 2. Below  $\sim 70$  hPa, the cooling is similar to that of Figure 1 in the southern hemisphere and northern low latitudes, with statistical significance again obtained in the Antarctic region. This suggests that ozone changes are the primary cause of the cooling of these regions. Above this altitude, the inclusion of WMGGs yields increased cooling (or reduced warming), with the magnitude of temperature change being comparable to or exceeding that due to ozone loss; the vertical extent of the middle and upper stratospheric warming at  $60$ – $90\text{S}$  is also greatly reduced. The area of statistical significance in Figure 2 extends throughout the low and midlatitude stratosphere above  $\sim 70$  hPa in both experiments. Again, virtually the entire northern polar stratosphere exhibits no statistically significant change in either experiment.

### 4. Comparisons With Observed Trends

[11] The global and annual-mean vertical profile of the simulated temperature trends are compared with the observed trends in Figure 3; the modeled and observed trend uncertainties are also shown. The observations indi-

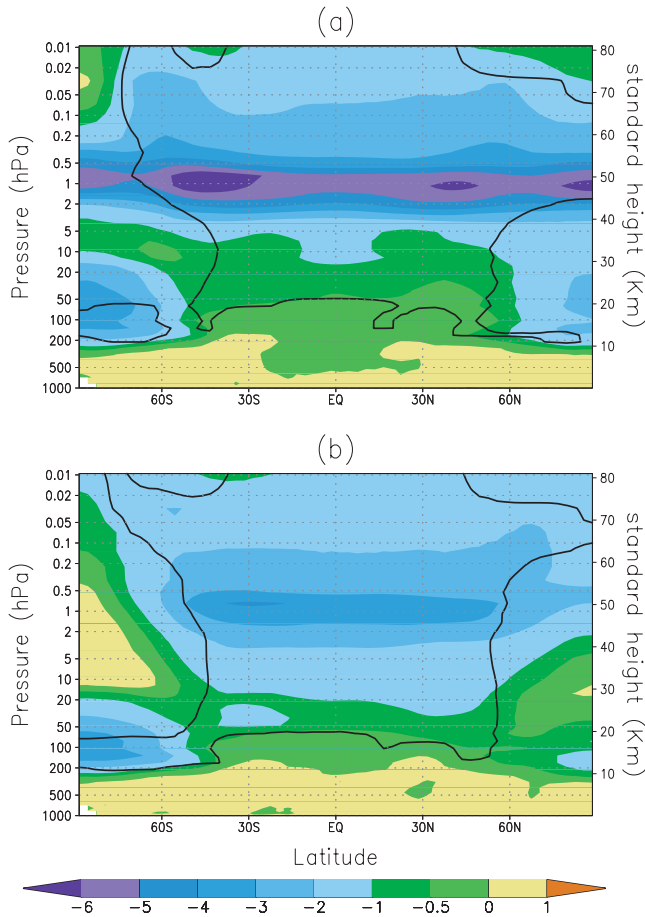


**Figure 2.** Same as Figure 1, except for ozone + WMGG change experiments (a) A2 and (b) B2.

cate a statistically significant cooling trend at all stratospheric altitudes. The combined ozone and WMGG simulations yield a statistically significant cooling over the entire stratosphere. At 50–100 hPa, all four simulations yield temperature trends that are within the uncertainty estimates, with the simulated mean value less than that observed. The global-mean lower stratosphere trends are dominated by ozone and are rather insensitive to the ozone base climatology employed in this study. In the middle stratosphere, model-simulated trends are affected substantially by WMGGs. In the 10–30 hPa region, the A2 and B2 simulations agree well with observations, whereas the ozone-only simulations yield insufficient cooling. Curiously, the A2 and B2 simulations overestimate the observed trend at  $\sim 5$  hPa, while the ozone-only results are slightly more consistent with the observed profile.

[12] Above 5 hPa, both ozone and WMGGs contribute to the observed cooling. Here, the effects of differing ozone base climatologies become important, with trends in Set B being  $\sim 1$ – $1.5$  K/decade less in magnitude than those in Set A. In the 1–3 hPa region, the B2 simulation yields the best agreement with observations; since the model’s 2-sigma variability in this region is  $\sim 0.2$ K, the result indicates that both ozone and WMGG trends must be included to account for the observed trends. Both Set A and B simulations yield a peak cooling at  $\sim 1$  hPa, thus failing to mimic the observed increase in cooling trend right up to 0.5 hPa. This

result is also evident in the L and RS ozone-only studies; inclusion of WMGGs here does not alter this feature. Note that ozone losses are not known above 50 km and hence not accounted for in this study.

[13] The zonal, annual-mean trends in the lower stratosphere from the simulations (pressure-weighted average of 50–100 hPa values) and satellite observations are compared in Figure 4. For comparison purposes, the RSR result is also illustrated; that study employed an idealized ozone trend profile constrained by observations of the 1980s decadal column ozone trend. For convenience, only the results of the A2 and B2 experiments are considered. The observations indicate a statistically significant cooling trend in the  $\sim 20$ – $70$ N region and poleward of  $\sim 20$ S, with the variability being least in the midlatitudes. The simulated trends are consistent with the observations (to within model and observational uncertainties) in the southern hemisphere, tropics and high northern latitudes. In high southern latitudes, the modeled trends are similar to SSU measurements but exceed the MSU estimate; this difference could be due in part to the sensitivity of the trend to the heights sampled by the instruments since, in the Antarctic, the region of cooling is immediately below a region of warming (Figure 2; also R01). The simulations also exhibit a cooling trend in the northern polar region (especially in A2), but the absence of significance inhibits a definitive inference. In northern midlatitudes, the model trends are smaller than observations. Inclusion of water vapor trends could enable a better agreement of the mean estimate [Forster and Shine, 1999; Smith et al., 2001], although uncertainty in ozone loss and

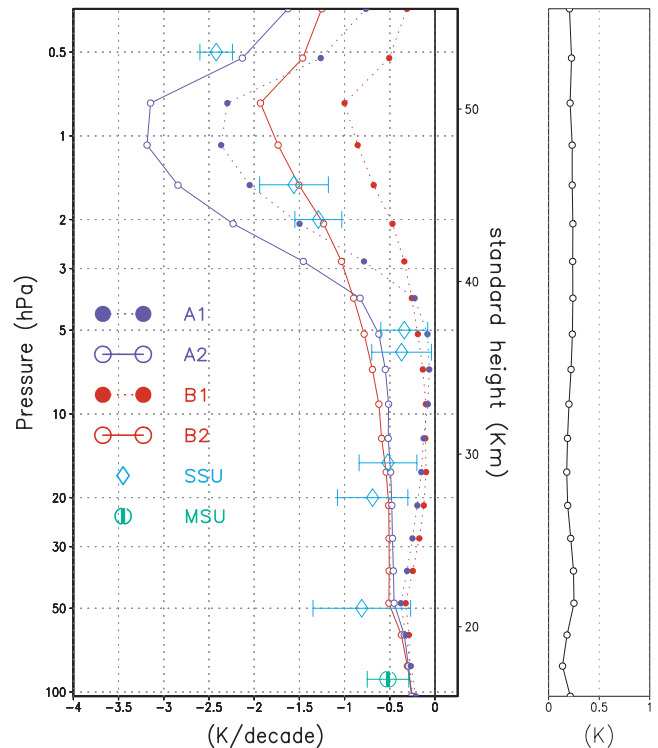


**Figure 3.** Vertical profile of the global, annual-mean temperature trend (1979–2000) from satellites (MSU, SSU) and model results. Horizontal bars denote 2-sigma observational uncertainties. The right panel shows the model’s 2-sigma interannual variability.

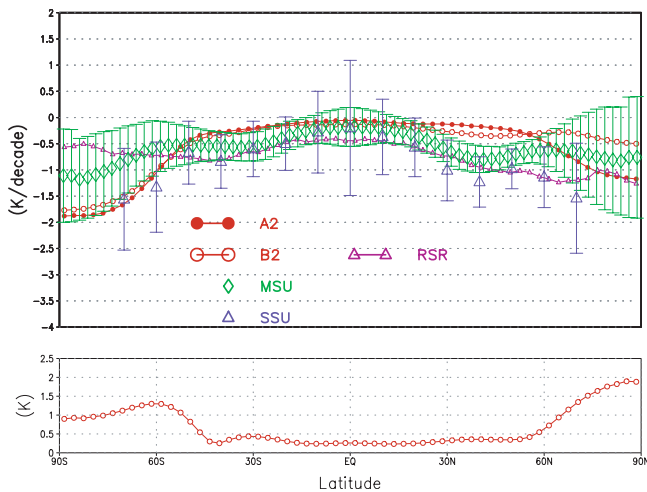


**Figure 4.** Zonal, annual-mean lower stratospheric temperature trend (1979–2000) from satellites (MSU, SSU) and model results (A2 and B2). Vertical bars denote 2-sigma observational uncertainties. RSR denotes a model simulation of the effect due to the 1980s ozone loss (see text). The lower panel shows the model's 2-sigma interannual variability.

biases in the model's dynamical response cannot be excluded. The RSR simulation for the 1980s ozone loss had a larger cooling trend than A2 and B2 in low and middle latitudes, due to its assumption of a larger ozone loss in the lowermost region of the lower stratosphere.

## 5. Discussions

[14] This study indicates that the global-and-annual-mean temperature change observed in the stratosphere is well-simulated using the best available knowledge of both ozone and WMGG changes and of the background ozone (FK) climatology. Since global-and-annual-mean stratospheric temperature changes are primarily consequences of the externally applied radiative perturbations, the agreement between the B2 simulation and observations implies that changes in ozone plus WMGGs are the responsible radiative factors accounting for a major portion of the observed cooling trend in the global-mean stratosphere over the past two decades.

[15] The combined ozone and WMGG perturbation yields statistically significant temperature trends over a broad region of the low-to-midlatitude stratosphere above  $\sim 70$  hPa as well as in a substantial portion of the Antarctic lower stratosphere. In the lower stratosphere, the simulated cooling trends in the global-mean, southern hemisphere and northern low latitudes arise mainly due to ozone change and do not depend greatly on the choice of the background ozone climatology. WMGGs contribute increasingly to the stratospheric cooling above  $\sim 70$  hPa. The upper stratospheric temperature response depends on both ozone and WMGG changes; the response shows a marked sensitivity to the base ozone climatology employed. This identifies it as an important factor in biases and calls attention to development of robust climatologies for perturbation studies. The relative role of ozone and WMGGs, as diagnosed here at different altitudes, indicates the desirability of performing GCM investigations of trends over the entire stratosphere.

[16] The zonal-mean model simulations of the lower stratosphere trends agree quantitatively with the observations (within uncertainty limits) except for an underestimate of the cooling at the northern midlatitudes. This agreement builds upon results from previous ozone-only simulations (L, RS) showing similar consistency. The results reinforce strongly the inference (e.g. R01) of the large role due to ozone loss in the observed lower stratospheric temperature trends during the 1980s as well as the 1990s. The lack of a statistical significance in the northern polar stratosphere makes attribution arguments for that region a difficult proposition.

[17] The equilibrium model simulations here have used a perturbed ozone profile, derived from a linear ozone trend, in which the influences of natural variability have been removed. As a further study, it would be interesting to test whether simulations of the effects of trace gases on the interannual variations in temperature exhibit as good an agreement with observations as is the case for the recent decadal trends. Water vapor increases [Forster and Shine, 1999; Smith et al., 2001] and any uncertainty in ozone changes near the tropopause would influence the simulated trends and could improve the agreement with observations to an even greater extent than here.

[18] **Acknowledgments.** We are grateful to the SPARC Stratospheric Temperature Trends Assessment group for the stratospheric temperature trends data and to Bill Randel for the ozone data.

## References

- Fels, S. B., J. D. Mahlman, M. D. Schwarzkopf, and R. W. Sinclair, Stratospheric sensitivity to perturbations in ozone and carbon dioxide: Radiative and dynamical response, *J. Atmos. Sci.*, **37**, 2265–2297, 1980.
- Forster, P. M. de F., and K. P. Shine, Stratospheric water vapor changes as a possible contributor to observed stratospheric cooling, *Geophys. Res. Lett.*, **26**, 3309–3312, 1999.
- Fortuin, P., and H. Kelder, An ozone climatology based on ozonesonde and satellite measurements, *J. Geophys. Res.*, **103**, 31,709–31,734, 1998.
- Hansen, J. E., H. Wilson, M. Sato, R. Ruedy, K. Shah, and E. Hansen, Satellite and surface temperature data at odds?, *Clim. Change*, **30**, 103–117, 1995.
- IPCC, *Climate Change 1995: The Science of Climate Change. Intergovernmental Panel on Climate Change*, J. T. Houghton et al., ed., Cambridge Univ. Press, New York, 1996.
- Labitzke, K., and H. van Loon, A note on the distribution of trends below 10 hPa: The extratropical Northern Hemisphere, *J. Meteor. Soc. of Japan*, **73**, 883–889, 1995.
- Lacis, A. A., and J. E. Hansen, A parameterization for the absorption of solar radiation in the earth's atmosphere, *J. Atmos. Sci.*, **31**, 118–133, 1994.
- Langematz, U., An estimate of the impact of observed ozone losses on stratospheric temperature, *Geophys. Res.*, **27**, 2077–2080, 2000.
- Mahlman, J. D., J. P. Pinto, and L. J. Umscheid, Transport, radiative, and dynamical effects of the antarctic ozone hole: a GFDL "SKYHI" model experiment, *J. Atmos. Sci.*, **51**, 489–508, 1994.
- Ramachandran, S., V. Ramaswamy, G. Stenchikov, and A. Robock, Radiative impact of the Mount Pinatubo volcanic eruption: Lower stratospheric response, *J. Geophys. Res.*, **105**, 24,409–24,429, 2000.
- Ramaswamy, V., M. D. Schwarzkopf, and W. Randel, Fingerprint of ozone depletion in the spatial and temporal pattern of recent lower-stratospheric cooling, *Nature*, **382**, 616–618, 1996.
- Ramaswamy, V., et al., Stratospheric temperature trends: Observations and model simulations, *Reviews of Geophysics*, **39**, 71–122, 2001.
- Randel, W. J., and F. Wu, A stratospheric ozone trends data set for global modeling studies, *Geophys. Res. Lett.*, **26**, 3089–3092, 1999.
- Rosier, S. M., and K. P. Shine, The effect of two decades of ozone change on stratospheric temperature, as indicated by a general circulation model, *Geophys. Res. Lett.*, **27**, 2617–2620, 2000.
- Smith, C., J. Haigh, and R. Toumi, Radiative forcing due to trends in stratospheric water vapor, *Geophys. Res. Lett.*, **28**, 179–182, 2001.